

Advanced Sensor and Target Development to Support Robot Accuracy Degradation Assessment

Guixiu Qiao, *Senior Member, IEEE*

Abstract— This paper presents a vision-based, 6 degree of freedom (DOF) measurement system that can measure robot dynamic motions in real-time. A motorized target is designed as a part of the system to work with a vision-based measurement instrument, providing unique features to stand out from the background and enable the achievement of high accuracy measurement. With the capability to measure a robot's 6 DOF information, the robot's accuracy degradation can be monitored, assessed, and predicted to avoid a costly, unexpected shutdown, or decrease in manufacturing quality and production efficiency. The National Institute of Standards and Technology (NIST) is developing the necessary measurement science to support the monitoring, diagnostics, and prognostics of robot systems by providing intelligence to enhance maintenance and control strategies. The robot accuracy degradation research includes the development of modeling and algorithm for the test method, advanced sensor and target development to accurately measure robot 6 DOF information, and algorithms to analyze the data. This paper focuses on the development of the advanced sensor and target. A use case shows the use of the measurement system on a Universal Robot to support the robot accuracy degradation assessment.

I. INTRODUCTION

Robots are known for their repeatability, but more accurate robots have become valuable tools to enable broader robot applications [1-4]. For example, more off-line programming can be performed because robots can move to desired positions precisely with improved absolute accuracy [2]. Also, many new robot applications such as robot material removal, high precision assembly, robotic drilling, robot riveting, and robot metrology require robots with high accuracy [5-7]. Compared to expensive solutions which use custom machines, high accuracy robots with articulated arms can extend arm to cover a relatively large work volume and can navigate along curvature surfaces or into tight spaces. Implementing robots in manufacturing processes benefits manufacturers by improving flexibility and reducing costs.

As more robotic technologies are integrated into complex manufacturing environments, it is critical to understand a robot system's reliability [10]. A manufacturing system's efficiency, quality, and productivity compromise can be comprised by the robot's accuracy degradation. Robot accuracy degradation is relatively difficult to be detected compared to the hard stop of a production line [8, 9]. Although the robot's performance is degraded, the robot is still running, and parts are making. However, the robot is working at a decreased level of performance. Moreover, a robot's accuracy

degradation may also influence other automation components' performance. For example, stresses and strains may accumulate when a fixture or a gripper is working constantly in a biased position. The accumulated stresses and strains may result in the mechanical failure or wear of the fixture or gripper. It is very challenging to decouple errors and find the root causes of failures caused by robot accuracy degradation.

To assess robot accuracy degradation, the deviations of the robot's motion need to be measured. Fig. 1 shows a robot's

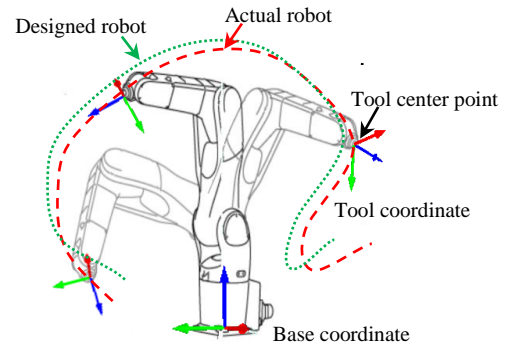


Fig. 1. Robot tool center point

actual motion has deviated from the designed motion. Moreover, the deviations are different at different locations within the robot's workspace. To determine the deviation, a sensor is needed to measure the x, y, z, pitch, yaw, and roll of the robot tool center point (TCP). As shown in Fig. 1, TCP is located at the end of a robot's kinematic chain. Any error in the robot kinematic chain will be reflected as a deviation of the TCP position and orientation. There is a wide range of techniques being used to measure and calibrate robots. These techniques include: 1) Pose matching methods via driving a robot to a known location, and the pose calculated by the robot controller being recorded [10]; 2) Polar measurement techniques with laser trackers or total stations [11]; 3) Trilateration with a theodolite, using cable potentiometer systems, or laser interferometers [12]; 4) Tactile techniques using gauges or coordinate measurement machines [13]; 5) Inertial navigation systems and magnetic field systems [14]; 6) Photogrammetry with high-resolution digital systems [15-17].

Some of the above-mentioned measurement techniques involve rather expensive metrology instruments (e.g., laser trackers, total stations, etc.). Pose matching, gauges, or coordinate measurement machines are very slow. Trilateration and other methods usually lack orientation information. The vision-based system is gaining more attention in recent years. They have the advantages of being relatively low-cost and non-contact [18]. Innovations in new vision sensors (including low noise, high dynamic range, high resolution, and hardware-accelerated processing) are accelerating the

Guixiu Qiao is with the National Institute of Standards and Technology, Gaithersburg, MD 20899 USA (phone: 301-975-2865; fax: 301-990-9688 e-mail: guixiu.qiao@nist.gov).

application of vision-based systems [19]. For these reasons, a pilot study on the applicability of a dual camera stereo system based on low-cost vision hardware components to industrial robot health assessment tasks was conducted. This study focused on aspects of accuracy and real-time processing.

The measurement of the TCP deviation is the first step to assess robot accuracy degradation. A robot's TCP deviation varies at different locations. Even at the same location, if the robot approaches the location from different directions, the TCP deviations are different. Therefore, there is an infinite number of combinations of locations and directions. It is impossible to measure all possible combinations to determine the overall accuracy of the robot. There needs to be a methodology to efficiently measure, monitor, diagnose, predict, and maintain the health of a robot (collectively known as Prognostics and Health Management (PHM)).

The National Institute of Standards and Technology (NIST) is working to develop the measurement science in assessing robot health and optimizing the maintenance of robot systems. As a subset of this research, a quick health assessment methodology was developed to enable manufacturers to quickly assess a robot's accuracy degradation throughout the robot workspace [20]. This paper focuses on the advanced sensor and target development to support the robot's health assessment by examining the degradation of the robot TCP accuracy. The following sections present the design principle of the new target that exceeds the existing target representation; analyze the accuracy and real-time processing capability; show the design of the system; and present a use case of using the system on a Universal Robot to support the accuracy degradation assessment methodology.

II. DESIGN PRINCIPLE OF 3 DOF AND 6 DOF REPRESENTATION

Any possible movement of a rigid body can be expressed as a combination of the basic 6 DOF - 3 translations and 3 rotations. Translation has 3 degrees of freedom: forward/back, up/down, left/right. Rotation has 3 degrees of freedom: pitch, yaw, and roll. A measurement system usually contains the measurement instrument (or sensor) and a measurement target. The measurement target defines what features can be captured by the measurement instrument to represent 3 DOF or 6 DOF information.

The 3 DOF translation is usually represented as a fixed point (x, y, z) on an object. Because once the (x, y, z) is defined, the object is not free to translate in any direction. When the object moves, its translation can be measured via measuring the position changes of the point on the object. If a measurement system can measure a point, the measurement system can measure the 3 DOF information of the object. Fig. 2 (a) to (d) are examples of 3 DOF targets used by vision-based measurement instruments. Fig. 2 (a) is a light-emitting diode (LED) target. It can only be viewed when the LED target is facing the measurement instrument. The output is the center position (x, y, z) of the LED target. Fig. 2 (b) shows sphere targets used by photogrammetric systems. A sphere target is a target that can be measured from any view. The sphere center is the (x, y, z) position to be measured. A photogrammetric system captures the two dimensional (2D)

image of the sphere target. The centroid of the 2D image is detected and later triangulated to a 3 DOF point that represents the sphere center. Fig. 2 (c) is an example of the sphere target used by scanning systems. A scanning system scans the surface of the sphere and outputs a point cloud. A sphere surface is constructed using a best-fit method. Then the center of the sphere is calculated. Fig. 2 (d) is the other type of 3 DOF target used by vision-based systems. The intersection corner of the checkerboards is the point being measured.

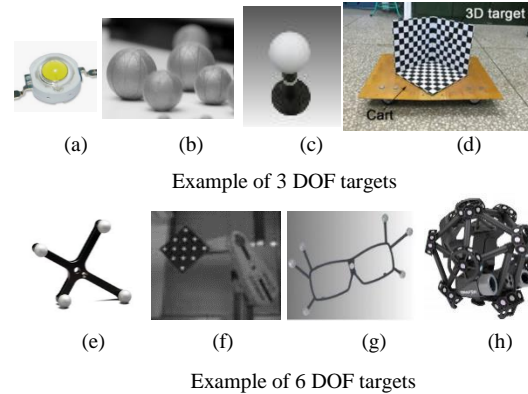


Fig. 2. 3 DOF and 6 DOF target representation

Besides translation, many applications also need rotation information. When the 3 degrees of rotation is added to the translation, a coordinate frame is formed. The origin of the coordinate frame represents the point where translation is measured. Positional tracking can be performed by tracking the origin position. To define rotation, three axes of the coordinate frame are used. They are: a primary axis, a secondary axis, and a tertiary axis. In Fig. 1, the tool frame is made up of the three axes at the TCP. The tool center point is the origin of the frame. The tool coordinate is programmable and can be "taught" for each tool or fixture attached to the robot. Any error in the kinematic chain will be reflected as the TCP error. Measuring the 6 DOF errors of the tool frame is a measure of robot accuracy. If a measurement system can measure a coordinate frame, the measurement system can measure the 6 DOF information of the object.

Existing 6 DOF target representation can be created by combining multiple 3 DOF targets. One representation that has been widely used to define a coordinate frame is using the three point method. A coordinate frame is defined using three points. A coordinate frame is represented by defining an origin and two axes. The third axis is perpendicular to the other two axes. The three points are used as: 1) a point defining the origin, 2) a point defining the primary axis, e.g., X-axis; this axis is formed by creating a vector from the origin pointing to the point, and 3) a point in a plane, e.g., XY plane. The secondary axis is in this XY plane. It is defined by a vector that starts from the origin and is perpendicular to the X-axis. The third point is used to define the secondary axis's positive direction. Examples of 6 DOF targets are shown in Fig. 2 (e) to (h). In Fig. 2 (e) and (f), multiple spheres use a planar layout to construct a coordinate frame. More than three sphere targets are implemented to create redundancy. The need for redundancy is to avoid image overlapping when viewing the target from different viewpoints. In Fig. 2 (g), spheres use a spatial layout to construct a frame. Fig. 2 (h) shows a complex

LED spherical array. It combined multiple LEDs to create a 6 DOF target.

For robot accuracy degradation assessment task, a measurement system needs to perform accurate measurements and measure the TCP's 6 DOF information while the robot is stationary or moving. A novel measurement system is developed at NIST to achieve high accuracy and high speed 6 DOF measurements. A dual-camera measurement instrument and a smart target construct a measurement system. The following sections of the paper describe its accuracy and real-time process potential by analyzing the feature detection uncertainty and coordinate frame construction uncertainty.

III. NEW TARGET DEVELOPMENT

NIST developed a 6 DOF measurement system was developed to perform the assessment of the industrial robot accuracy degradation. The system consists of a measurement instrument with two high-speed color cameras and a smart target as shown in Fig. 3. The smart target is mounted at the end of the robot arm. The vision-based measurement instrument is mounted on a tripod and placed on the floor facing the robot. A measurement software was developed to take measurements of robot TCP position and orientation.

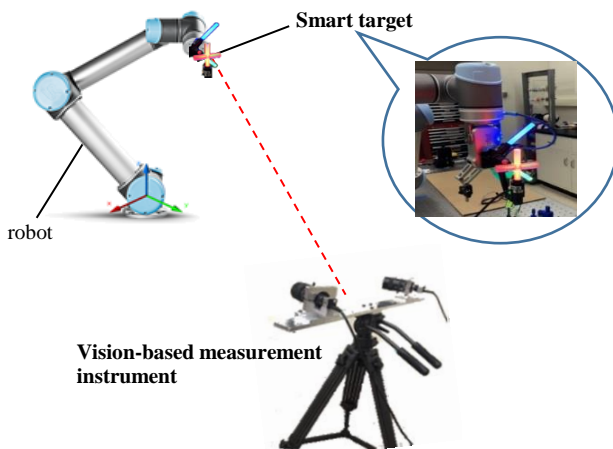


Fig. 3. Sensor and target development to support robot accuracy degradation assessment

The vision-based system is used for the measurement system because: (1) A vision-based system is a non-contact measurement system that can capture both position and orientation simultaneously; (2) High accuracy measurement (with sub-pixel accuracy) has been enabled by novel camera and image processing technology; and (3) A vision-based system is relatively cost-effective to integrate [18] with the mature of camera technology. Color images provide redundant information to get more accurate target detection. The use of high-speed camera and real-time computation enable high-speed measurements. The output of the measurement is $(x, y, z, \text{pitch}, \text{yaw}, \text{and roll})$ of a moving object with high accuracy.

The smart target is protected under a U.S. provisional patent. It contains light pipes illuminated in three colors. The 6 DOF information is represented by a coordinate frame. As shown in Fig. 4, two cylindrical light pipes form an intersection that represents the origin. The coordinate frame of the smart target is shown in Fig. 4 (a). The two intersecting

light pipes are mounted on two motorized rotation axes. The two rotary axes are motorized. Driven by inertial measurement sensors, the intersection pipes can rotate constantly so that the target Y axis points towards the measurement instrument. This creates a constant line-of-sight between the target and the measurement system, even when the target is moving. On the bottom of the smart target, the directions of the x and y axes are defined by two different color light pipes. Fig. 4 (b) shows the smart target mounted on the robot end effector. Fig. 4 (c) shows the light pipe images as seen by the camera when the light pipes are illuminated.

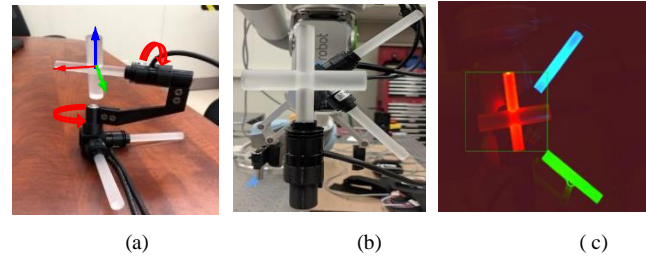


Fig. 4. Smart target developed at NIST

IV. ANALYSIS ON ACCURACY AND REAL-TIME PROCESSING CAPABILITY

To analyze the accuracy of the 6 DOF representation, the sources of measurement uncertainty need to be known. The 3/6 DOF measurement is a mix of hardware and software to detect the position (and orientation) of an object. A vision-based measurement instrument takes images of the target, performs image processing to capture features, and finally outputs the measurement result in either 3 or 6 DOF. Two major concerns of vision-based measurement systems are accuracy and real-time processing capability. Existing targets have different uncertainties in the detection of features when the target is at different distances or at different poses. These uncertainties influence the accuracy of the final measurement. Also, ambient light has strong effects on the image quality and affects the robustness and accuracy. When the target is in an industrial environment with a complex background, the ability to isolate the target from the background influences the efficiency of real-time processing to track a moving object.

A. Uncertainty calculation for feature detection

Features are components used to construct a coordinate frame. A point feature is a basic feature to represent the translation or the origin of a coordinate frame. The uncertainty of the point feature detection influences the final measurement accuracy. A very common target artifact to define a point is a sphere target. The sphere target can be measured from different views and the derived sphere center is a point feature.

The roundness of the sphere target and the evenness of the surface influence the result of the sphere center detection. For example, Fig. 2 (b) shows the reflective spheres used by infrared cameras. The sphere roundness can be well controlled by machining. However, to make a sphere reflect infrared radiation (IR) light, there are two methods to create the target. The more accurate method is to apply the coating with reflective material. It is expensive in manufacturing because the manufacturing process needs high accuracy in coating control. Reflective tape can be wrapped around a sphere to create the reflective sphere target. It is challenging to

control the roundness of the wrapped spherical. Thus, this kind of target can be used for moderate accuracy applications.

The calculation of sphere centers also has many uncertainties. For scanning systems, since the output of the sphere surface is point cloud, the best-fit method is used to construct the sphere. The sphere center is then calculated. If the point cloud consists of the whole sphere surface, the sphere center can be accurate. But in real situations, only a partial sphere surface will be captured. The best-fit result is biased in this condition. Moreover, the uncertainty varies when measuring the sphere from a different view. For photogrammetric systems, the sphere target is captured as 2D images which are circular on the camera sensors. The centroid of the circle needs to be calculated. The centroid detection accuracy is influenced significantly by the image quality, such as the image exposure, image focus, and the number of the image pixels that represent the target in the camera sensor. The ambient light also has a strong influence on the uncertainty of sphere center detection.

The smart target developed at NIST does not use a sphere to define the coordinate origin. Instead, line features are used. Two perpendicular lines form a “cross”. The intersection of the lines defines the coordinate frame origin. The line features are created using cylindrical light pipes. The dimension of the light pipe artifact is 10 mm in diameter and 75 mm long. Three colors of LEDs are used in the smart target design with special wavelengths that match with the narrow band filters on the measurement instrument’s cameras. The purpose is to reduce the effects of ambient light. With special surface finishing, the entire cylindrical surface has an even light distribution. Fig. 5 shows the image of light pipe artifacts representing line features.



Fig. 5. Light pipe artifacts of smart target for line feature representation

B. Uncertainty calculation for coordinate frame construction

After the basic features are detected, they are used to construct a coordinate frame. When using sphere targets to construct a coordinate frame, one of the sphere centers is selected as the origin. The problem of this method is: the origin definition inherits the uncertainty from the sphere center measurement in the scale of one-to-one.

For axis definition, the axis of a coordinate frame is defined using two points (two sphere centers) – the origin and a point on the axis. Fig. 6 shows the axis definition error caused by point detection uncertainty. P_0 is the origin point. P_1 is the true position of the second point. P_1' is the real P_1 position with Δ error caused by the uncertainty of point P_0 and P_1 . The angular error of the axis definition is $\tan^{-1}(\Delta / p_0p_1)$. Even a small positional error of the point (Δ) can cause a large angular error of the axis vector.

For the same Δ error, a shorter distance between P_0 and P_1 corresponds to a larger angular error. In Fig. 6, P_2' has the

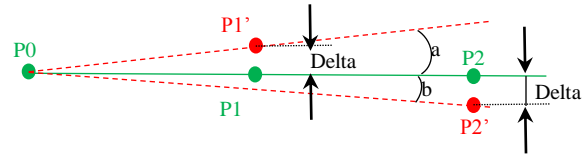


Fig. 6. Axis definition error caused from point detection uncertainty

same Δ error, but the angular error a is bigger than the angular error b because P_1 is closer to P_0 than P_2 . Therefore, to achieve higher accuracy, the target needs to be larger to maximize the distance $\overline{p_0p_1}$. However, it is not practical to build a very large target. As a result, for a target that uses two/multiple spheres to define the axis, the measurement has larger angular uncertainties than a target using line features.

Besides the direct definition of a coordinate frame, some technologies use the best-fit method to find the transformation between the same points measured in two coordinate frames. Fig. 7 (a) shows a group of points in one coordinate frame and Fig 7. (b) shows the same point group in another coordinate frame. The point group in Fig. 7 (b) is transformed to the coordinate frame in Fig. 7 (a), and the best-fit result is shown in Fig. 7(c). Best-fit usually uses the method of minimizing the sum of the squares of the offsets as the cost function. This method eliminates the one-to-one error propagation from the point detection to the final result. However, the best-fit method only minimizes the translation deviation. Angular errors are not minimized and are, therefore, less accurate.

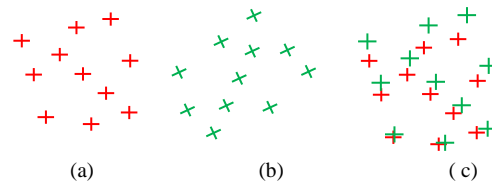


Fig. 7. Uncertainty of sphere center

To avoid these problems, the smart target uses line targets instead of sphere targets. Cylindrical artifacts are used to create line features. The center line of the cylindrical artifact used in the smart target defines an axis. Fig. 8 shows an example of line construction. Since more points are used to fit the axis line, the accuracy of the line detection is much higher compared with the method of defining an axis using two sphere centers. Also, with more points used to fit the line, algorithms can filter out outliers for better line construction. Additionally, the light pipe consists of extra features including color, width, edge features, etc. They can be used to improve the accuracy of target detection. Moreover, best-fit can output multiple results for best-fit data analysis, including straightness, error distribution, error pattern, etc. The best-fit straightness of the line can be used as an important factor to monitor the camera lens distortion. If the straightness of the line fitting results shows distortion, the camera and lens need to be checked. The design of the smart target enables the on-site self-checking capability of the measurement system.

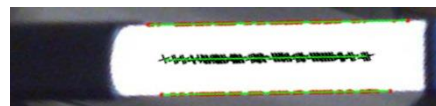


Fig. 8. Center line construction image for a cylinder artifact

C. Method to stand out an object from the background

The lighting condition in an industrial environment is complex. Various light sources, including ceiling lights, light towers for safety systems, and LED indicators on fixtures, may influence the image quality of the vision-based measurement system. A widely used technology to make a target stand out in a complex background is the utilization of infrared (IR) technology. The shortcoming of this method is the images contain only the markers. When ambient lights exist in the environment, the reflected light from ambient objects will be treated as real targets. There is no redundancy to judge if the detected target is a fake target when applications are used in a complex industrial environment.

To avoid the shortcoming of IR images, high-speed color cameras were selected for the measurement system developed at NIST. Fig. 9 shows the color image of the smart target. The smart target uses three colors of LEDs to illuminate the light pipes. The wavelength combination of the three colors is used as the “signature” of the smart target. Using this “signature”, the target can be quickly identified from the complex background. Once the target is found, a bounding box is defined surrounding the target and will be constantly tracked when the target moves with the robot arm. The camera will use a feature of Area of Interest (AOI). It allows a camera using a small AOI window size to operate at higher frame rates compared with one using a full frame capture. Since a smaller window size requires less calculation time compared to a full window size, more complex algorithms can be applied to achieve more robust and accurate results. Fig. 9 (a) shows that the smart target was identified. Fig. 9 (b) shows that the cross center was detected to define the coordinate frame origin. Fig. 9 (c) shows the axis line is detected even when the ceiling light is within the view of the cameras. The color information is used to speed up the calculation and provide more redundancy in the algorithms, for example, avoidance of fake target detection. Advanced color image processing (e.g., pattern reorganization) techniques are utilized to get more accurate target detection results. A graphics processing unit (GPU) technique is used to accelerate the image processing for real-time measurement. The output of the measurement is (x , y , z , pitch, yaw, and roll) of a moving object.

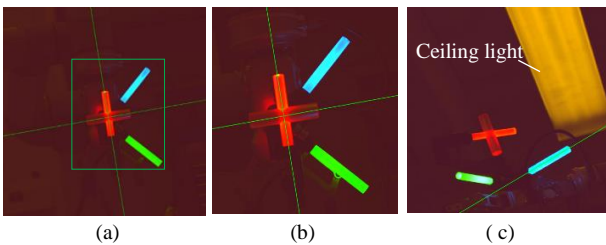


Fig. 9. Color image of the smart target

In summary, besides the advantages in accuracy improvements, the measurement system has advantages in solving the following challenges required for robot dynamic accuracy assessment. These challenges include:

1) Dynamic measurement

Since the smart target measures 6 DOF, every snap of the smart target gives the position and orientation. The high-speed camera can take 175 frames per second in full frame mode. The camera speed can be increased further when using the

camera AOI mode to track the small area around the target, allowing the dynamic movement of the robot to be captured.

2) Non-blocking measurement design

Traditional targets have an image overlapping problem. The target may block itself in some poses. The smart target is motorized by rotating on two rotary gimbals. The target always rotates towards the measurement system. This eliminates self-blocking and yields optimized pose for measurement.

3) Unique definition of a coordinate frame

Traditional spherical targets can use any sphere as the origin. It is hard to find the coordination definition when multiple coordinates exist in a system. The 6 DOF smart target uses the cross center as the origin and other two light pipes as the axis direction. This creates a consistent frame definition.

V. USE CASE DEVELOPMENT

A quick health assessment methodology is developed at NIST. The purpose is to assess the robot accuracy degradation throughout the robot workspace. The quick health assessment methodology includes: 1) development of a sensor and target to measure the robot (x , y , z , pitch, yaw, and roll of the TCP); 2) a robot error model to represent the robot’s geometric and non-geometric errors; 3) a test method to define the robot movements; and 4) algorithms to process the measured data to assess the robot’s health status. In the quick health assessment methodology, step 2) develops an error model to represent a robot’s deflections of the robot’s structure and joints, the ideal and non-ideal motion of joints. Step 3) generates a measurement plan that satisfies the requirements to support the robot error model identification. The robot is commanded to move based on the measurement plan. The movements are measured by the advanced sensor and target. Measurement data is fed to the algorithm developed in step 4) to assess the robot health and predict the failure of robot operations under the current accuracy status [9].

The developed measurement system is used to acquire the robot TCP 6 DOF information. As shown in Fig. 10 (a), the smart target is mounted at the end of a Universal Robot arm. The cross light pipe is motorized to constantly rotate toward the camera instrument as shown in Fig. (a). The vision-based measurement instrument is mounted on a tripod and set up at the opposite end of the robot. Fig. 10 (b) shows the measurement plan generated for the Universal Robot. The measurement plan requires the robot TCP to move throughout the entire workspace. The motions distribute evenly in both joint space and Cartesian space. The even distribution of sampling prevents the analysis algorithm from missing errors or too heavily weighting errors, which will bias the results. The coverage of the overall joint space and Cartesian space means that the measurement plan will exercise the robot beyond a partial range of joints or work zones. The coverage of overall joint space enables the capture of joint performance through the full motor and encoder ranges. Covering the entire workspace enables the evaluation of various rigidity conditions. To minimize potential interruptions during robot motion and measurement, a collision check is made during the measurement plan generation process. Also, a line-of-sight check is performed to ensure the planned positions do not occlude the target from the measurement instrument, i.e., arm blocking the target. The output of the measurement system is x , y , z , pitch, yaw, and roll.

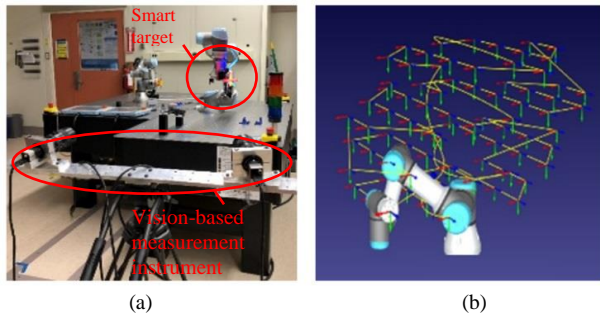


Fig. 10. Robot quick health

The TCP 6 DOF measurements are the input of the test method model and the analysis algorithms. The test method model builds a robot error model that can represent a robot's position dependent, non-geometric errors. A novel algorithm is developed to solve the robot error model that contains hundreds of unidentified parameters [9]. A method is developed to decouple the uncertainties of the measurement instrument from the actual robot errors. The analysis outputs the accuracy degradation assessment results.

The quick health assessment can be used to swiftly detect degradations in robot accuracy by finding the robot pose deviations from the nominal poses. The methodology provides manufacturers a tool to quickly detect problems in scenarios when the environmental conditions have changed, reconfigurations are needed, or a critical task is about to perform. The quick health assessment methodology can help to reduce unexpected shutdowns, and help optimize the maintenance strategy to improve productivity via monitoring the robot performance degradation.

VI. SUMMARY

This paper presents the development of an advanced sensor and target to assess robot accuracy degradation. The sensor and target (U.S. patent pending for the smart target) are featured with novel designs that differ from and exceed the performance of existing vision-based measurement systems, especially with respect to accuracy and real-time processing potential. The use of line features enables the high accuracy measurement of the 6 DOF information. The smart target can be utilized in a variety of applications. These applications include registering multiple machines/tools/objects, adaptively locating objects during mobile operations, and precisely tracking the pose of an object. This paper also presents a use case for using the measurement system in assessing robot accuracy degradation. Future efforts are underway to develop additional industrial use cases for applications that require high-precision motions.

NIST DISCLAIMER

Certain commercial entities, equipment, or materials may be identified in this document in order to illustrate a point or concept. Such identification is not intended to imply recommendation or endorsement by NIST, nor is it intended to imply that the entities, materials, or equipment are necessarily the best available for the purpose.

REFERENCES

[1] A. D. Pham and H. J. Ahn, "High precision reducers for industrial robots driving 4th industrial revolution: state of arts, analysis, design, performance evaluation and perspective," *International Journal of Precision Engineering and Manufacturing-Green Technology*, vol. 5, pp. 519-533, Aug 2018.

[2] M. Placzek and L. Piszczek, "Testing of an industrial robot's accuracy and repeatability in off and online environment," *Eksplotacja I Niezawodnosc-Maintenance and Reliability*, vol. 20, pp. 455-464, 2018.

[3] H. J. Kim, A. Kawamura, Y. Nishioka, and S. Kawamura, "Mechanical design and control of inflatable robotic arms for high positioning accuracy," *Advanced Robotics*, vol. 32, pp. 89-104, 2018.

[4] D. Culla, J. Gorrotxategi, M. Rodriguez, J. B. Izard, P. E. Herve, and J. Canada, "Full Production Plant Automation in Industry Using Cable Robotics with High Load Capacities and Position Accuracy," in *Robot 2017: Third Iberian Robotics Conference*, Vol 2. vol. 694, A. Ollero, A. Sanfeliu, L. Montano, N. Lau, and C. Cardeira, Eds., ed Cham: Springer International Publishing Ag, 2018, pp. 3-14.

[5] D. D. Chen, P. J. Yuan, T. M. Wang, Y. Cai, and L. Xue, "A Compensation Method for Enhancing Aviation Drilling Robot Accuracy Based on Co-Kriging," *International Journal of Precision Engineering and Manufacturing*, vol. 19, pp. 1133-1142, Aug 2018.

[6] A. Drouot, R. Zhao, L. Irving, D. Sanderson, and S. Ratchev, "Measurement Assisted Assembly for High Accuracy Aerospace Manufacturing," *IFAC Papersonline*, vol. 51, pp. 393-398, 2018.

[7] A. Klimchik and A. Pashkevich, "Robotic manipulators with double encoders: accuracy improvement based on advanced stiffness modeling and intelligent control," *IFAC Papersonline*, vol. 51, pp. 740-745, 2018.

[8] G. Liu, "Control of robot manipulators with consideration of actuator performance degradation and failures," in *2001 IEEE International Conference on Robotics and Automation*, Vols I-IV, Proceedings, 2001, pp. 2566-2571.

[9] G. X. Qiao and B. A. Weiss, "Quick health assessment for industrial robot health degradation and the supporting advanced sensing development," *Journal of Manufacturing Systems*, vol. 48, pp. 51-59, Jul 2018.

[10] Y. Wu, A. Klimchik, S. Caro, B. Furet, and A. Pashkevich, "Geometric calibration of industrial robots using enhanced partial pose measurements and design of experiments," *Robotics and Computer-Integrated Manufacturing*, vol. 35, pp. 151-168, Oct 2015.

[11] Y. B. HuangFu, L. B. Hang, W. S. Cheng, L. Yu, C. W. Shen, J. Wang, et al., "Research on Robot Calibration Based on Laser Tracker," in *Mechanism and Machine Science*. vol. 408, X. Zhang, N. Wang, and Y. Huang, Eds., ed Singapore: Springer-Verlag Singapore Pte Ltd, 2017, pp. 1475-1488.

[12] I. A. Sultan and J. G. Wager, "Simplified theodolite calibration for robot metrology," *Advanced Robotics*, vol. 16, pp. 653-671, 2002.

[13] N. Zaimovic-Uzunovic and S. Lemes, "Cylindricity Measurement on a Coordinate Measuring Machine," in *Advances in Manufacturing*, A. Hamrol, O. Ciszak, S. Legutko, and M. Jurczyk, Eds., ed Cham: Springer International Publishing Ag, 2018, pp. 825-835.

[14] E. Pivarciova, P. Bozek, Y. Turygin, I. Zajack, A. Shchenyatsky, S. Vaclav, et al., "Analysis of control and correction options of mobile robot trajectory by an inertial navigation system," *International Journal of Advanced Robotic Systems*, vol. 15, p. 15, Jan 2018.

[15] B. Diewald, R. Godding, and A. Henrich, *Robot calibration with a photogrammetric online system using reseau-scanning-cameras* vol. 2252. Bellingham: Spie - Int Soc Optical Engineering, 1994.

[16] J. Peipe, *Photogrammetric performance evaluation of digital camera backs for in-studio and in-field use* vol. 2598. Bellingham: Spie - Int Soc Optical Engineering, 1995.

[17] A. Fillion, A. Joubair, A. S. Tahan, and I. A. Bonev, "Robot calibration using a portable photogrammetry system," *Robotics and Computer-Integrated Manufacturing*, vol. 49, pp. 77-87, Feb 2018.

[18] M. Švaco, B. Šekoranja, F. Šuligoj, and B. Jerbić, "Calibration of an Industrial Robot Using a Stereo Vision System," *Procedia Engineering*, vol. 69, pp. 459-463, 2014.

[19] R. Ahmad and P. Plapper, "Safe and Automated Assembly Process using Vision Assisted Robot Manipulator," *Procedia CIRP*, vol. 41, pp. 771-776, 2016.

[20] G. Qiao, C. Schlenoff, and B. A. Weiss, "Quick positional health assessment for industrial robot prognostics and health management (PHM)," in *2017 IEEE International Conference on Robotics and Automation (ICRA)*, 2017, pp. 1815-1820.